Three-dimensional optimal perturbations in viscous shear flow

Kathryn M. Butler and Brian F. Farrell
Division of Applied Sciences, Harvard University, Cambridge, Massachusetts 02138

(Received 28 May 1991; accepted 6 April 1992)

Transition to turbulence in plane channel flow occurs even for conditions under which modes of the linearized dynamical system associated with the flow are stable. In this paper an attempt is made to understand this phenomena by finding the linear three-dimensional perturbations that gain the most energy in a given time period. A complete set of perturbations, ordered by energy growth, is found using variational methods. The optimal perturbations are not of modal form, and those which grow the most resemble streamwise vortices, which divert the mean flow energy into streaks of streamwise velocity and enable the energy of the perturbation to grow by as much as three orders of magnitude. It is suggested that excitation of these perturbations facilitates transition from laminar to turbulent flow. The variational method used to find the optimal perturbations in a shear flow also allows construction of tight bounds on growth rate and determination of regions of absolute stability in which no perturbation growth is possible.

I. INTRODUCTION

Despite decades of research, the problem of transition to turbulence in a shear flow has yet to be fully resolved. Turbulence develops in laboratory plane Poiseuille flow at Reynolds numbers, based on half-channel length and maximum velocity, as low as 1000[1] or as high as 8000,[2] depending on the level of noise in the experiment. In plane Couette flow, turbulence has been encountered at Reynolds numbers as low as 360.[3] Classical linear theory, based on the existence of exponential temporal modal instability, predicts a critical Reynolds number of $R_c \simeq 5772$ for Poiseuille flow and stability for all values of R in Couette flow, predictions clearly at variance with observations.

The nature of the disturbances which appear in shear flow is also incompletely explained by traditional instability theory. Squire's theorem[4] applied to a viscous flow requires every unstable three-dimensional (3-D) modal disturbance to be associated with a more unstable two-dimensional (2-D) modal disturbance at a lower Reynolds number. This result has been widely interpreted as reducing the problem of finding sufficient criteria for instability, and therefore the minimum critical Reynolds number, to an investigation of two-dimensional disturbances. However, the variations that are most often observed in a viscous shear flow tend to take the form of streaks oriented in the streamwise direction. In the experiments of Klebanoff *et al.*,[5] spacers were added to control these spanwise variations since they could not be eliminated. Over the course of several years of experiments with forced Tollmien–Schlichting waves, Nishioka and his co-workers were unable to eliminate spanwise distortion of the basic flow[6] despite techniques which reduced noise levels in the incoming fluid to under 0.05%.

The possibility of transient growth of disturbances in viscous flow has been recognized for over a century.[7] Recently, the initial value problem has attracted the attention of researchers studying transition to turbulence in viscous shear flows. The justification of these "bypass" approaches, so named because they bypass the ideas of traditional instability theory, is the speculation that transition may result if some initial disturbances arising from the finite level of noise present in any flow are able to grow sufficiently to activate nonlinear mechanisms or to provide new basic states for secondary instabilities. These disturbances are sometimes called "algebraic instabilities" to distinguish them from exponential instabilities.

For inviscid flows, Ellingsen and Palm[8] demonstrated that the streamwise velocity grows linearly with time for a disturbance with no streamwise variation. Given a basic velocity $U(y)$ in the x direction, the linearized momentum equation for the streamwise velocity component u is

$$\frac{\partial u}{\partial t} + vU' = 0, \tag{1}$$

where the prime indicates a derivative in y. The mean momentum is transported by the wall normal velocity of this disturbance. Because the normal velocity v is independent of time, the streamwise velocity increases linearly with time. This growth mechanism has been labeled lift-up[9] and vortex stretching, although it is more accurately referred to as vortex tilting, as can be shown by linearizing the inviscid vorticity equation,

$$\frac{\partial \boldsymbol{\omega}}{\partial t} + \mathbf{u}\cdot\nabla\boldsymbol{\omega} = \boldsymbol{\omega}\cdot\nabla\mathbf{u}. \tag{2}$$

For a disturbance independent of the x direction, linearization leaves only a vortex-tilting term,

$$\frac{\partial \omega}{\partial t} = -U'\frac{\partial v}{\partial z}, \tag{3}$$

where ω is the normal vorticity component and $-U'$ is the vorticity of the mean flow, which is in the cross-stream z direction. This mean z vorticity is tilted into the y direction by the perturbation strain rate $\partial v/\partial z$, giving rise to the increase of y vorticity.

Landahl[10] has shown that inviscid shear flows support three-dimensional disturbances whose energy grows at

 0899-8213/92/081637-14$04.00 © 1992 American Institute of Physics

least linearly in time as they lengthen in the streamwise direction. The large horizontal velocities generated over time by these disturbances are due to the above-described vortex-tilting mechanism. In his studies of localized disturbances in plane Poiseuille flow, Henningson[11] demonstrated that as a certain simple disturbance evolves it develops a streaky character and becomes dominated by effects due to vortex tilting. The same is true for a simple disturbance developing on a flat-plate boundary layer, as observed through both analysis and experiment by Breuer and Haritonidis.[12]

In addition to the vortex-tilting mechanism, another growth mechanism exists for shear flows, as can be seen from the inviscid energy density equation,

$$\frac{\partial \mathscr{E}}{\partial t} = -\frac{1}{2}\int_{-1}^{1} U'\overline{uv}\, dy, \tag{4}$$

where $\mathscr{E}$ is perturbation energy density and the overbar denotes an average in x. This expression indicates that a disturbance can extract energy from the mean shear by transporting momentum down the mean momentum gradient through the action of perturbation Reynolds stress. To visualize this mechanism more clearly, note that the energy increases when

$$\frac{\partial \psi}{\partial x}\frac{\partial \psi}{\partial y}U' = \left(\frac{\partial \psi/\partial x}{\partial \psi/\partial y}\right)\left(\frac{\partial \psi}{\partial y}\right)^2 U' = -\left(\frac{\partial y}{\partial x}\right)_{\psi}\left(\frac{\partial \psi}{\partial y}\right)^2 U' \tag{5}$$

is positive over the integral. As perturbation streamlines with an initial phase tilt opposite that of the mean shear, indicated by $(\partial y/\partial x)_{\psi}U' < 0$ in (5), are advected by the mean shear into a more upright orientation, the perturbation gains energy. As the shear continues to advect the disturbance, its phase becomes tilted in the opposite direction, indicated by $(\partial y/\partial x)_{\psi}U' > 0$, and the disturbance energy is returned to the mean flow.[13] An investigation of two-dimensional perturbations which grow the most in L_2 and energy norms for plane Poiseuille and Couette flow carried out by Farrell[14] showed the Reynolds stress mechanism to be responsible for rapid transient growth in exponentially stable two-dimensional viscous shear flow.

Resonance theory has been used to find initial perturbations that grow rapidly in time. Direct resonances between a single Orr–Sommerfeld mode, which is coupled with normal vorticity in the three-dimensional equations, and a single Squire mode have been found in Couette flow,[15] Poiseuille flow,[16] and boundary layers.[17–19] The presence of a direct resonance introduces an algebraic growth term into the temporal development of a disturbance, although the disturbance may still decay in time.[20] By solving the linear initial-value problem in plane Poiseuille flow, Gustavsson[21] found that the energy of an initial three-dimensional disturbance consisting of one of the least-stable Orr–Sommerfeld modes with zero initial vorticity was capable of large transient growth before the onset of decay.

In a flow subject to stochastic forcing, disturbances may arise that are configured in such a way that they are able to gain energy from the mean flow. If these disturbances attain sufficient amplitude, they may ultimately give rise to nonlinear equilibrated structures or turbulent patches. The search for transient growing perturbations can be rationalized by determining the initial conditions that gain the most energy over a specified time period. Such optimal perturbations indicate the disturbances that are most likely to be found in a stochastically driven flow, and set tight bounds on the growth capability of all perturbations.

The same variational techniques used by Farrell[14] to find the two-dimensional optimal perturbations in a viscous shear flow can be applied to the three-dimensional equations for normal velocity and normal vorticity to determine the three-dimensional disturbances that grow the most on chosen time scales.[22] In this work, these optimal perturbations are studied for Couette, Poiseuille, and Blasius shear flow profiles.

II. VARIATIONAL PROBLEM

Consider a plane channel with steady mean flow $U(y)$ in the streamwise (x) direction. The evolution of small three-dimensional perturbations to this flow is governed by the linearized Navier–Stokes and continuity equations:

$$\left(\frac{\partial}{\partial t}+U\frac{\partial}{\partial x}\right)u + U'v = -\frac{\partial p}{\partial x}+\frac{1}{R}\Delta u, \tag{6a}$$

$$\left(\frac{\partial}{\partial t}+U\frac{\partial}{\partial x}\right)v = -\frac{\partial p}{\partial y}+\frac{1}{R}\Delta v, \tag{6b}$$

$$\left(\frac{\partial}{\partial t}+U\frac{\partial}{\partial x}\right)w = -\frac{\partial p}{\partial z}+\frac{1}{R}\Delta w, \tag{6c}$$

$$\frac{\partial u}{\partial x}+\frac{\partial v}{\partial y}+\frac{\partial w}{\partial z}=0, \tag{7}$$

where $R = U_0 h/\nu$ is the Reynolds number, U_0 is the maximum velocity, h is the channel half-width, ν is the kinematic viscosity, Δ is the three-dimensional Laplacian, and $(') \equiv d/dy$. Time is nondimensionalized by the advective time scale h/U_0. The no-slip boundary conditions are $u = v = w = 0$ at $y = \pm 1$. The mean flow profile is $U = y$ for Couette flow and $U = 1 - y^2$ for Poiseuille flow.

Manipulation of this system of equations results in a system for two variables, normal velocity v and normal vorticity $\omega = \partial u/\partial z - \partial w/\partial x$:[15]

$$\left(\frac{\partial}{\partial t}+U\frac{\partial}{\partial x}\right)\Delta v - U''\frac{\partial v}{\partial x}-\frac{1}{R}\Delta\Delta v = 0, \tag{8a}$$

$$\left(\frac{\partial}{\partial t}+U\frac{\partial}{\partial x}\right)\omega - \frac{1}{R}\Delta\omega = -U'\frac{\partial v}{\partial z}, \tag{8b}$$

with boundary conditions $v = \partial v/\partial y = \omega = 0$ at $y = \pm 1$. Flow variables u, w, and p can be calculated using the relationships:

$$\left(\frac{\partial^2}{\partial x^2}+\frac{\partial^2}{\partial z^2}\right)u = \frac{\partial \omega}{\partial z}-\frac{\partial^2 v}{\partial x\,\partial y}, \tag{9}$$

$$\left(\frac{\partial^2}{\partial x^2}+\frac{\partial^2}{\partial z^2}\right)w = -\left(\frac{\partial \omega}{\partial x}+\frac{\partial^2 v}{\partial z\,\partial y}\right), \tag{10}$$

$$\left(\frac{\partial^2}{\partial x^2}+\frac{\partial^2}{\partial z^2}\right)p=\left(\frac{\partial}{\partial t}+U\frac{\partial}{\partial x}-\frac{1}{R}\Delta\right)\frac{\partial v}{\partial y}-U'\frac{\partial v}{\partial x}, \quad (11a)$$

or

$$\Delta p=-2U'\frac{\partial v}{\partial x}. \quad (11b)$$

Assume a solution in the form

$$v(x,y,z,t)=\tilde{v}(y)\exp[i(\alpha x+\beta z)+\sigma t], \quad (12a)$$

$$\omega(x,y,z,t)=\tilde{\omega}(y)\exp[i(\alpha x+\beta z)+\sigma t], \quad (12b)$$

with the understanding that only the real parts of these quantities will be used when considering physical values. The following eigenproblem for $\tilde{v}$ and $\tilde{\omega}$ results:

$$\{-i\alpha U\Delta+i\alpha U''+[\Delta(\Delta)/R]\}\tilde{v}=\sigma\Delta\tilde{v}, \quad (13a)$$

$$[-i\alpha U+(\Delta/R)]\tilde{\omega}-i\beta U'\tilde{v}=\sigma\tilde{\omega}, \quad (13b)$$

with $\Delta=d^2/dy^2-k^2$ and $k^2=\alpha^2+\beta^2$.

The equation for $\tilde{v}$ is the classical Orr–Sommerfeld equation, whose solutions include the two-dimensional Tollmien–Schlichting waves. For three-dimensional perturbations we must simultaneously solve the Orr–Sommerfeld equation and the normal vorticity equation, which is driven by the normal velocity.

The set of eigenmodes for this problem is discrete and complete for bounded flows.[23–25] We assume that we can approximate an arbitrary initial condition with fixed wave numbers α and β in the homogeneous streamwise and spanwise directions, respectively, by summing a sufficient number, $2N$, of eigenmodes:

$$v=\sum_{j=1}^{2N}\gamma_j[\tilde{v}_j\exp(\sigma_j t)]\exp[i(\alpha x+\beta z)], \quad (14a)$$

$$\omega=\sum_{j=1}^{2N}\gamma_j[\tilde{\omega}_j\exp(\sigma_j t)]\exp[i(\alpha x+\beta z)], \quad (14b)$$

where the coefficient γ_j represents the spectral projection on mode j.

The discretized Orr–Sommerfeld and normal vorticity equations take the form

$$\begin{bmatrix}\mathcal{L} & 0\\ \mathcal{C} & \mathcal{S}\end{bmatrix}\begin{bmatrix}\tilde{v}\\ \tilde{\omega}\end{bmatrix}=\sigma\begin{bmatrix}\tilde{v}\\ \tilde{\omega}\end{bmatrix}. \quad (15)$$

The Orr–Sommerfeld operator $\mathcal{L}$, Squire operator $\mathcal{S}$, and coupling operator $\mathcal{C}$ in this equation are

$$\mathcal{L}=\Delta^{-1}\{-i\alpha U\Delta+i\alpha U''+[\Delta(\Delta)/R]\}, \quad (16a)$$

$$\mathcal{S}=[-i\alpha U+(\Delta/R)], \quad (16b)$$

$$\mathcal{C}=(-i\beta U'), \quad (16c)$$

where the inverse Laplacian operator Δ^{-1} is rendered well posed by inclusion of appropriate boundary conditions. The eigenproblem is solved for all $2N$ eigenmodes at once. The eigenmodes that arise from this formulation include solutions of the coupled Orr–Sommerfeld/normal vorticity problem and solutions of the homogeneous normal vorticity equation, also known as Squire modes.

For self-adjoint operators, growth of any initial perturbation is simply a matter of tracking the individual growth of its orthogonal modes. What makes the initial-value problem for viscous shear flow interesting is that the set of operators involved is not self-adjoint in the norms of physical interest, including the energy norm. Although the modal analysis of an eigenproblem such as (15) is often referred to as the "normal mode" approach, the eigenfunctions resulting from a non-self-adjoint system are not orthogonal. As a result, a perturbation may consist of modes that initially destructively interfere, then separate in time to reveal considerable growth in integral energy or rms amplitude before decay and the eventual domination of the least-damped mode set in.

The non-self-adjoint nature of the three-dimensional problem in the L_2 norm is apparent from (15), which is non-self-adjoint whenever the coupling operator $\mathcal{C}$ is nonzero or either the Orr–Sommerfeld operator $\mathcal{L}$ or the Squire operator $\mathcal{S}$ (or both) is non-self-adjoint. It is apparent that (15) is self-adjoint in the limit $\alpha=0$ if $\mathcal{C}\equiv 0$ because both $\mathcal{L}$ and $\mathcal{S}$ become self-adjoint in this limit. Transient growth of perturbations has already been demonstrated for the two-dimensional problem, in which $\mathcal{C}=0$ and $\mathcal{L}$ is non-self-adjoint.[14,26] As we shall see, a nonzero coupling term can result in very strong growth even for perturbations in the limit $\alpha=0$, where the Orr–Sommerfeld and Squire operators become self-adjoint.

Given the possibility of transient perturbation growth in a viscous shear flow, it is of interest to determine the configuration which grows optimally in some sense. Development of the variational problem to obtain the optimal perturbations follows the approach taken by Farrell.[14] A norm to measure growth must first be chosen; we select the perturbation energy density as a physically interesting measure of perturbation magnitude. Assuming unit mass density, the kinetic energy density of a three-dimensional perturbation confined to a single wave number in the x and z directions is

$$\mathcal{E}=\frac{1}{2V}\int_{-1}^{1}\int_0^a\int_0^b(u^2+v^2+w^2)\,dz\,dx\,dy, \quad (17)$$

where $a=2\pi/\alpha$ and $b=2\pi/\beta$ are the wavelengths in x and z directions and $V=2ab$ is the integration volume. Velocities u, v, and w are physical quantities that are obtained by taking the real part of the complex quantities that we have been calculating; for example,

$$u=\mathrm{Re}\{\hat{u}(y,t)\exp[i(\alpha x+\beta z)]\}$$
$$=\tfrac{1}{2}\{\hat{u}\exp[i(\alpha x+\beta z)]+\hat{u}^*\exp[-i(\alpha x+\beta z)]\}. \quad (18)$$

Eliminating u^2+w^2 from (17) using (9) and (10) and integrating over x and z results in an expression for the energy density in terms of normal velocity v and normal vorticity ω:

$$\mathcal{E}=\frac{1}{8}\int_{-1}^{1}\left[\hat{v}^*\hat{v}+\frac{1}{k^2}\left(\frac{\partial\hat{v}^*}{\partial y}\frac{\partial\hat{v}}{\partial y}+\hat{\omega}^*\hat{\omega}\right)\right]dy. \quad (19)$$

To obtain the energy density in matrix form, we first rewrite the normal velocity and normal vorticity as

$$v=\mathbf{V}_t\gamma\exp[i(\alpha x+\beta z)],\quad V_{tmj}=\tilde{v}_{mj}\exp(\sigma_j t)$$

where (20)

$$\omega=\mathbf{\Omega}_t\gamma\exp[i(\alpha x+\beta z)],\quad \Omega_{tmj}=\tilde{\omega}_{mj}\exp(\sigma_j t).$$

The indices are m between 1 and N, referring to values at finite-difference locations $y_{m+1}=m\Delta y$, where $\Delta y=2/(N+1)$, and mode number j between 1 and $2N$. The spectral projection, γ, is a column vector indexed by the mode number j. The energy density can now be written in matrix form as

$$\mathscr{E}=\frac{\Delta y}{8}\left[\gamma^*\mathbf{V}_t^*\mathbf{V}_t\gamma+\frac{1}{k^2}\left(\gamma^*\frac{\partial\mathbf{V}_t^*}{\partial y}\frac{\partial\mathbf{V}_t}{\partial y}\gamma+\gamma^*\mathbf{\Omega}_t^*\mathbf{\Omega}_t\gamma\right)\right]$$

$$=\gamma^*\mathbf{E}_t\gamma. \tag{21}$$

The matrix $\mathbf{E}$ is Hermitian, and defines a positive definite quadratic form on the spectral projection γ.

The linear perturbation with wave numbers α and β that results in the maximum energy at time τ given unit initial energy can now be determined. This is a variational problem whose functional is

$$F=\gamma^*\mathbf{E}_\tau\gamma+\lambda(\gamma^*\mathbf{E}_0\gamma-1), \tag{22}$$

where λ is the Lagrange multiplier for the fixed initial energy. The Euler–Lagrange equation for this functional is

$$\mathbf{E}_\tau\gamma+\lambda\mathbf{E}_0\gamma=0, \tag{23}$$

a generalized eigenproblem whose eigenvalues λ are the ratios of energy at time τ to energy at time 0 corresponding to eigenvectors γ, the spectral projection of the perturbations associated with λ. Arranging the spectral projection in order of decreasing eigenvalue orders the necessarily orthogonal initial perturbations by energy growth over time τ. Note that optimal perturbations with wave numbers (α,β) will have the same growth as those with wave numbers $(\alpha,-\beta)$.

The eigenmodes of the linear dynamical system are only of interest to the optimal excitation problem in that they provide a convenient way to find the propagator[27] $\mathscr{R}(\tau,0)$ that moves initial conditions forward in time from 0 to τ:

$$\begin{bmatrix}\hat{v}(y,\tau)\\ \hat{\omega}(y,\tau)\end{bmatrix}=\mathscr{R}(\tau,0)\begin{bmatrix}\hat{v}(y,0)\\ \hat{\omega}(y,0)\end{bmatrix}. \tag{24}$$

In the context of this work, the modal decomposition plays no intrinsic role beyond that of providing a convenient representation of the propagator. Therefore, demonstrating convergence of $\mathscr{R}(\tau,0)$ is sufficient for our purposes. We note that there is an alternative approach to finding the propagator and its adjoint, without reference to modes, which involves numerical integration in time of the dynamic equations and the adjoint of the dynamic equations.[28]

The procedure for finding optimal perturbations is implemented using finite differences, and the QR algorithm is employed to solve the eigenproblems. A nine-point difference approximation for the Orr–Sommerfeld operator $\mathscr{L}$ was chosen through a comparison of Orr–Sommerfeld eigenvalues for Poiseuille flow to those obtained by Orszag.[29] Squire modes were verified by comparison to the temperature modes derived by Davey and Reid[30] for Couette flow, using the substitution suggested by Gustavsson and Hultgren.[15]

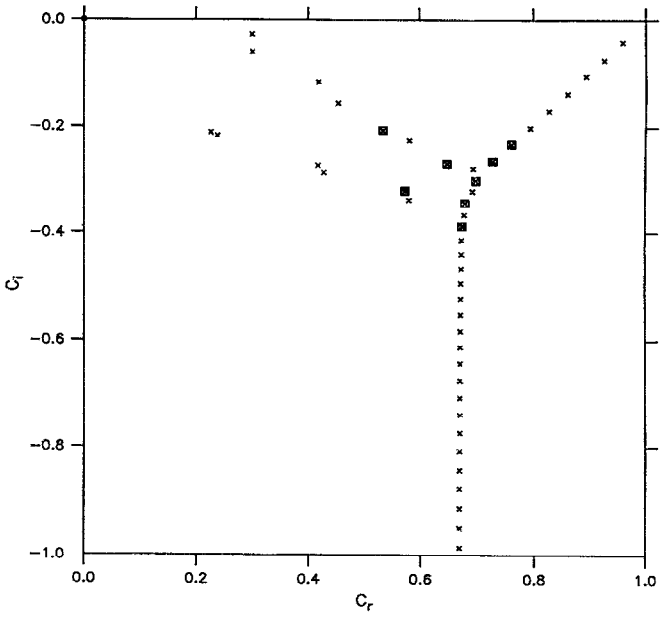

FIG. 1. Eigenvalues of the Orr–Sommerfeld equation for Poiseuille flow at $R=5000$, $\alpha=1.48$, and $N=199$, including both symmetric and antisymmetric modes. The eight modes whose eigenvalues are boxed contribute the most to the 2-D energy optimal with growth period $\tau=14.1$. Analysis of the pseudospectra for Poiseuille flow[26] shows that these antisymmetric modes nearest the intersection of A, P, and S branches have eigenvalues that are highly sensitive to perturbations, indicating near linear dependence of the eigenfunctions.

The Orr–Sommerfeld eigenvalues near the intersection of the A, P, and S branches for Poiseuille flow at $R=5000$ with discretization $N=49$ show the signature pattern for the finite-difference operator with low resolution.[31] Despite inaccuracies in the eigenvalues of certain individual modes, we find that as the discretization resolution is increased the representation (12) yields convergent propagators for representing the initial-value problem over the time scales of interest in this work. The maximum energy growth values reported in the tables are converged values from extrapolation at three levels of discretization between $N=48$ and 199.

The spectral projection γ for the two-dimensional optimal perturbation in Poiseuille flow shows that the Orr–Sommerfeld modes which are primarily represented in the composition of the optimal are the modes near the intersection of the A, P, and S branches, as indicated in Fig. 1. In a study of the pseudospectra of the Orr–Sommerfeld operator, Reddy *et al.*[26] identify the modes near this intersection as having eigenvectors that are nearly linearly dependent. The linear dependence of modes plays an important role in transient growth of disturbances in general and of disturbances in Poiseuille flow in particular.

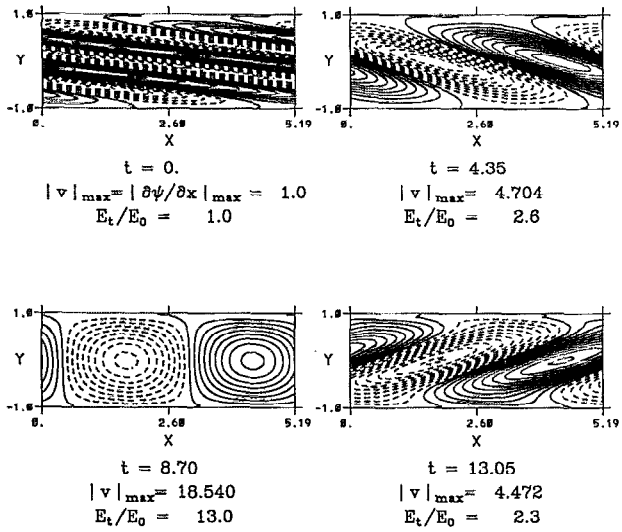

FIG. 2. Development of the perturbation streamfunction ψ for the best growing 2-D energy optimal in Couette flow with $R=1000$, located at $\alpha=1.21$, $\tau=8.7$. The streamfunction ψ is defined by $-\partial\psi/\partial y=u$ and $\partial\psi/\partial x=v$.

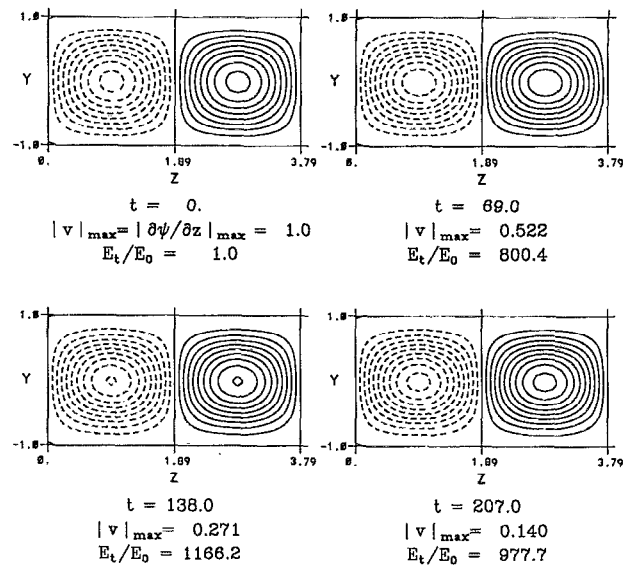

FIG. 3. Development of the perturbation streamfunction ψ for the best growing perturbation independent of x in Couette flow with $R=1000$, located at $\beta=1.66$, $\tau=138$. The streamfunction ψ is defined by $-\partial\psi/\partial y=w$ and $\partial\psi/\partial z=v$.

The optimal perturbations which are of interest include those capable of the greatest energy growth at a specified Reynolds number, those capable of the greatest growth rate, and those which define curves of specified energy growth. To locate these disturbances in (α,β,τ) space, drivers for finding a root given a bracketed interval and for maximizing a function in a single or multiple dimensions[32] were incorporated into the computer code.

III. OPTIMAL PERTURBATIONS IN COUETTE FLOW

We begin our search for linear perturbations that grow rapidly in a Couette flow by looking at the 2-D energy optimals previously investigated by Farrell.[14] Fixing the Reynolds number at $R=1000$ and the spanwise wave number at $\beta=0$, a search over streamwise wave numbers α and growth periods τ reveals that a 2-D perturbation with $\alpha=1.21$ grows the most, with energy increasing by a factor of 13 over $\tau=8.7$ advective time units. The development of the perturbation streamfunction shown in Fig. 2 demonstrates the down-gradient Reynolds stress mechanism of growth described in the Introduction.

The existence of a perturbation with energy growth of an order of magnitude in less than ten advective time units is impressive for a flow that does not support exponential instability at any Reynolds number. Now we shall see how much growth is possible from three-dimensional disturbances in the same flow.

The first 3-D disturbance we consider is one that does not vary in the downstream direction ($\alpha=0$). The maximum energy growth achievable by this type of disturbance, obtained using the variational method, is an increase by a factor of 1166, reached in 138 time units with $\beta=1.66$. The development of the streamfunction and streamwise velocity of this perturbation, shown in Figs. 3 and 4, respectively, make clear that this is a streamwise vortex. The growth of streamwise velocity streaks resulting from the vortex-tilting mechanism is stopped only by the effects of viscosity. When the normal velocity v is dissipated to levels at which the transport of momentum is unable to counter the dissipation of u, the disturbance begins to decay slowly. At this point, the streamwise velocity u has grown larger than v by a factor of order $O(R)$, with an attendant increase in energy, as pointed out by Kim and Moser.[33]

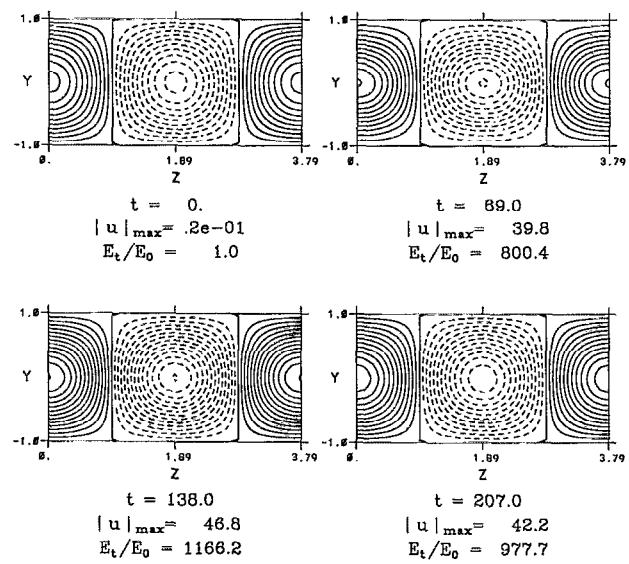

FIG. 4. Development of the perturbation streamwise velocity u for the best growing perturbation independent of x in Couette flow with $R=1000$, located at $\beta=1.66$, $\tau=138$. Values are normalized by the maximum value of v at time $t=0$.

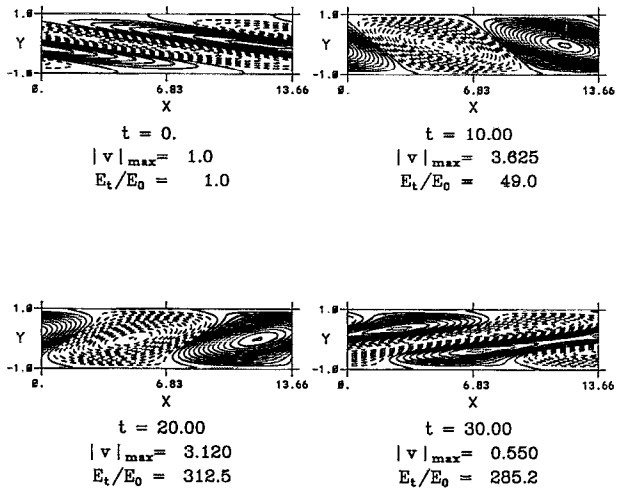

FIG. 5. Development of the normal velocity v at $z=0$ for the perturbation with maximum energy growth at $\tau=20$ in Couette flow with $R=1000$, located at $\alpha=0.46$, $\beta=1.9$.

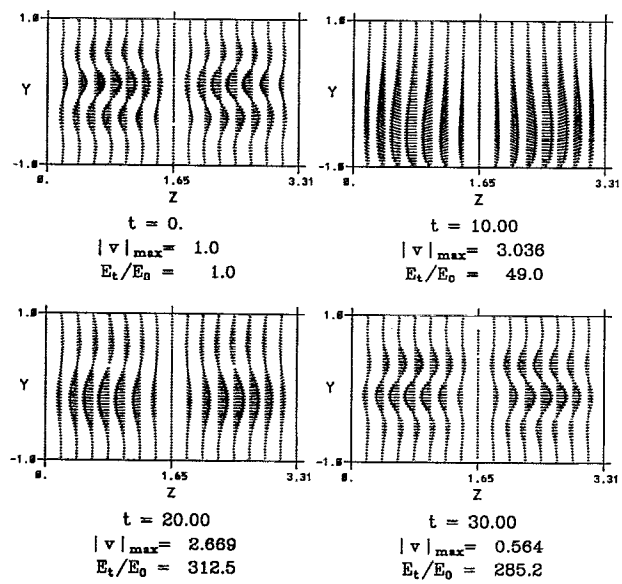

FIG. 6. Development of the velocities in the y-z plane at $x=0$ for the perturbation with maximum energy growth at $\tau=20$ in Couette flow with $R=1000$, located at $\alpha=0.46$, $\beta=1.9$.

Is it possible to find a disturbance with more growth potential than the streamwise vortex? A search for the global optimal for Couette flow at $R=1000$ using the variational method reveals a perturbation with $\alpha=0.035$ and $\beta=1.60$ that grows to 1185 times its initial energy in 117 time units. This perturbation primarily gains energy using the vortex-tilting mechanism, but obtains an additional increment of growth from the 2-D Reynolds stress mechanism (4) due to a favorable initial phase tilt opposite that of the mean shear. Its eventual decay is faster than that of the streamwise vortex because advection ultimately results in a phase orientation for which energy is transferred back into the mean flow by up-gradient Reynolds stress, an active decay mechanism.

We have seen that certain perturbations that are elongated in the streamwise direction have the potential to grow robustly in Couette flow. However, these perturbations require a rather long time to develop fully. It would also be interesting to determine the maximum growth that can be achieved on shorter time scales. Setting the growth period to $\tau=20$, corresponding to ten channel width advection times at the speed of the mean shear, a perturbation is found whose energy grows by a factor of 312. The best growth over five time units is 26 times the initial energy. These perturbations again grow by a combination of 2-D Reynolds stress and vortex-tilting mechanisms, with the 2-D mechanism becoming more important as the growth period becomes shorter.

The development of the strongest optimal at $\tau=20$ is illustrated in the cross sections shown in Figs. 5–7. Degenerate oblique perturbations with $\pm\beta$ are summed to symmetrize the perturbation in the y-z plane. The shorter streamwise length of this disturbance allows it to develop rapidly by taking advantage of the 2-D Reynolds stress mechanism (note the initial slant of the contours of v in Fig. 5) in addition to the vortex-tilting mechanism that causes the growth of u in Fig. 7.

Table I lists the values of growth period τ, wave numbers α and β, and energy growth at τ for each of the five cases described above. The energy growth with time of these optimals is plotted in Fig. 8. Note the greater rate of decay of the global optimal compared to the streamwise vortex, as described above, and the rapidity of short-term growth of the $\tau=20$ and $\tau=5$ optimals. The best two-dimensional optimal perturbation is seen to produce far

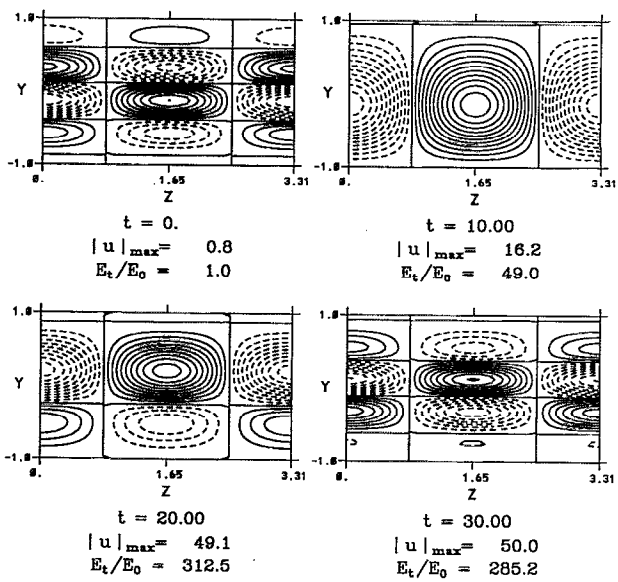

FIG. 7. Development of the perturbation streamwise velocity u at $x=0$ for the perturbation with maximum energy growth at $\tau=20$ in Couette flow with $R=1000$, located at $\alpha=0.46$, $\beta=1.9$. Values are normalized by the maximum value of v at time $t=0$.

TABLE I. Optimal perturbations in Couette flow at $R=1000$.

	τ	α	β	E_τ/E_0
Global optimal	117	0.035	1.60	1185
Best streamwise vortex	138	0	1.66	1166
Best optimal at $\tau=20$	20	0.46	1.9	312
Best optimal at $\tau=5$	5	1.6	2.9	26.4
Best 2-D optimal	8.7	1.21	0	13.0

less growth, indicative of the inappropriateness of interpreting Squire's theorem as placing a bound on general 3-D disturbance growth.

The trend of optimal perturbations to assume shorter streamwise wavelengths for growth on shorter time scales is illustrated in Fig. 9.

Recall that the solution of the energy growth eigenproblem results in $2N$ perturbations orthogonal in the energy inner product [cf. (21)], which are ordered in growth potential over a chosen time interval. If there are other types of perturbations whose growth approaches the best growing optimal, we would expect to occasionally see these perturbations in the laboratory. Figure 10 displays the first 50 eigenvalues, ordered in magnitude, from the eigenproblem for the Couette flow global optimal at $\alpha=0.035$, $\beta=1.60$. The second best optimal under these conditions grows by an order of magnitude less than the global optimal.

The global optima for Reynolds numbers from 31 to 4000 are listed in Table II. Note that the spanwise wave number for these disturbances is nearly constant at $\beta=1.6$, while in the streamwise direction the length increases as R for high Reynolds number flows. For highly viscous flows, the pure streamwise vortex is again the optimal. The time for maximum growth to occur increases as R, and the maximum energy growth is proportional to R^2. These relations are the same as those found by Gustavsson[21] for perturbations in Poiseuille flow forced by a single Orr–Sommerfeld mode.

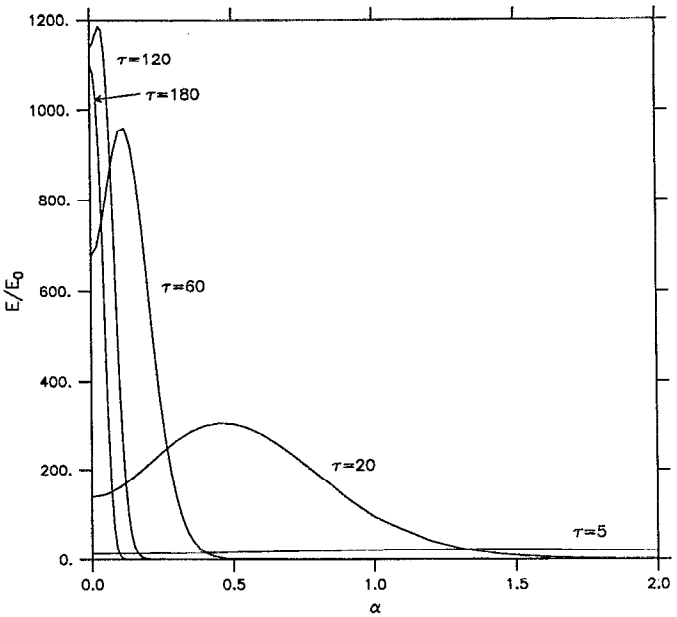

FIG. 9. Energy growth versus streamwise wave number α for optimal perturbations in Couette flow with $R=1000$ and fixed spanwise wave number $\beta=1.60$, illustrating the streamwise shortening of the best growing perturbations as the growth period decreases.

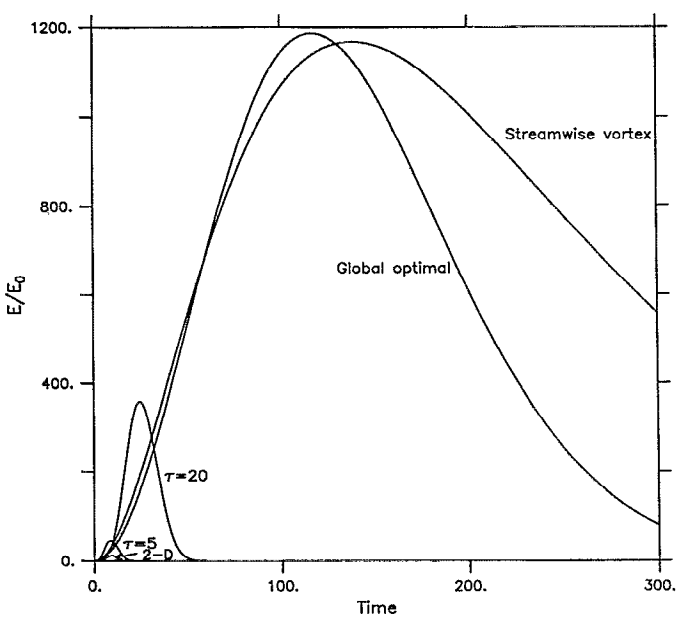

FIG. 8. Energy growth versus time for the global optimal, the streamwise vortex, and 2-D perturbation which grow the most, and perturbations which grow the most in 5 and 20 advective time units in Couette flow with $R=1000$.

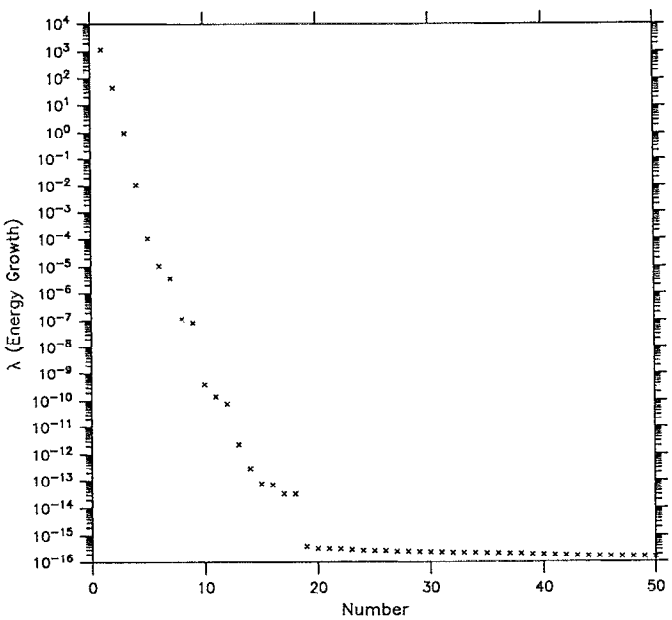

FIG. 10. Energy growth eigenvalues for the global optimal in Couette flow with $R=1000$, showing that the energy growth of the next most potent perturbation is smaller by an order of magnitude.

TABLE II. Global optima for Couette flow.

R	τ	α	β	E_τ/E_0
4000	467	0.0088	1.60	18 956
2000	234	0.0175	1.60	4739
1000	117	0.035	1.60	1184.6
500	59	0.067	1.60	296.0
250	30.2	0.12	1.61	73.9
125	16.1	0.144	1.63	18.55
62.5	8.2	0.0024	1.65	4.87
31.25	3.21	0	1.62	1.50

The highly streaky disturbances that gain the most energy in Couette flow will not develop nonlinearly into turbulence on their own.[21] However, streamwise vortices have been observed by Yang[34] and Hamilton[35] to undergo secondary instability leading to transition when the vortex Reynolds number, defined as

$$R_v=\Gamma/2\pi\nu, \tag{25}$$

where Γ is the vortex circulation and ν is the kinematic viscosity, exceeds a value of roughly 10. If transition to turbulence occurs when an initially small disturbance grows to an amplitude $O(1)$, perhaps instigating secondary instabilities leading to breakdown, then the smallest disturbance energy that would make transition possible at a given Reynolds number can be estimated by the reciprocal of the energy growth for the global optimum, and the disturbance root mean square velocity required for transition would be proportional to $1/R$.

Another subject of interest is the maximum rate of energy growth of a small perturbation in a flow. The energy method[36,37] was used by Howard[38] to determine the following bound for the energy growth of an arbitrary disturbance:

$$\frac{1}{\mathscr{E}}\frac{d\mathscr{E}}{dt}\leqslant\left(2\lambda-\frac{2m}{R}\right), \tag{26}$$

where $-\lambda$ is the lower bound for the most negative eigenvalue of the deformation rate tensor of the basic flow, $D_{ij}\equiv\frac{1}{2}(\partial U_i/\partial x_j+\partial U_j/\partial x_i)$, and m is the minimum of the functional $F=\langle|\nabla\mathbf{u}|^2\rangle/\langle|\mathbf{u}|^2\rangle$. For Couette flow, $\lambda=1/2$ and $m=(\pi/2)^2$.

A stronger bound on the minimum critical Reynolds number was determined by Joseph[39] by solving the variational problem

$$\frac{1}{R_c}=\max_{\mathbf{u}}\frac{-\int u_i u_j D_{ij}\,d\mathbf{x}}{\int(\partial u_i/\partial x_j)^2\,d\mathbf{x}} \tag{27}$$

for arbitrary fields $\mathbf{u}$ satisfying $\nabla\cdot\mathbf{u}=0$ in the volume and $\mathbf{u}=0$ on the boundaries. The least eigenvalue of this problem is $R_c=20.66$, which is associated with a disturbance varying only in the y-z plane whose spanwise wave number is $\beta=1.56$.

By looking for optimal perturbations which grow the most on a very short time scale ($\tau=0.01$ and 0.001 were used in practice), we can determine the most rapidly growing perturbation for any Reynolds number. This defines a constructive bound on energy growth, which is plotted in

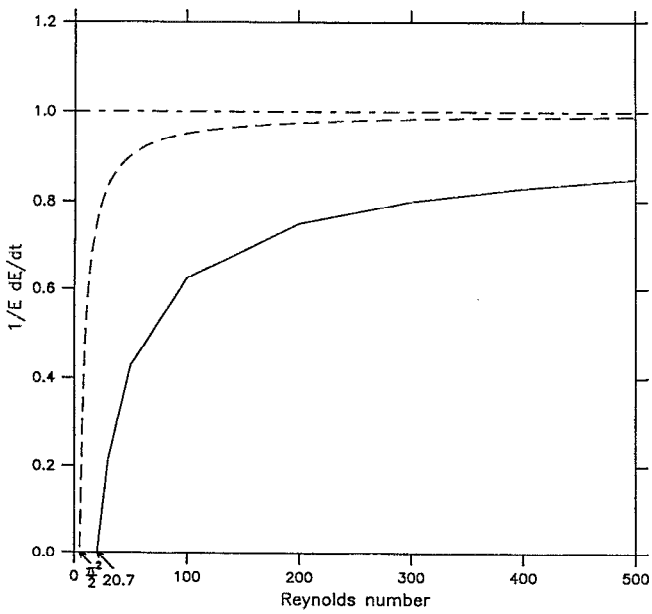

FIG. 11. Energy growth rate bounds for Couette flow. The solid line is the constructive bound on energy growth rate determined by optimal excitation techniques, the dashed line is Howard's energy integral bound, and the line at 1.0 is the absolute upper bound on energy growth rate. The optimal excitation curve meets the lower axis at $R=20.7$, the minimum critical Reynolds number found by Joseph.

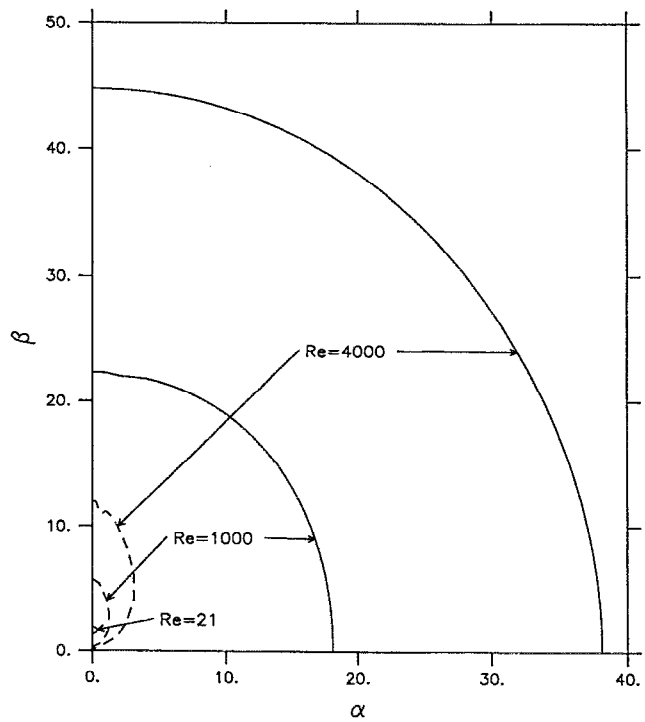

FIG. 12. Zero growth curves (solid) for Couette flow with $R=21$, 1000, and 4000, and 100× growth curves (dashed) for $R=1000$ and 4000. The zero growth curve for $R=21$ encloses the streamwise vortex with $\beta=1.56$ associated with Joseph's minimum critical Reynolds number.

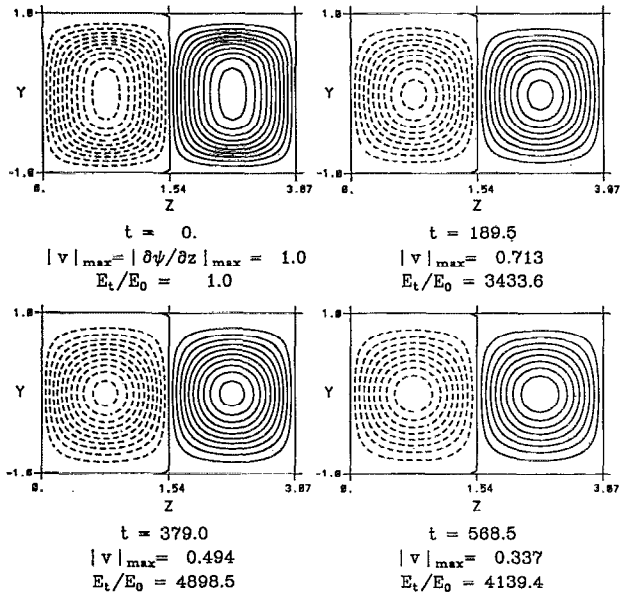

FIG. 13. Development of the perturbation streamfunction ψ for the global optimal in Poiseuille flow with $R=5000$, located at $\alpha=0$, $\beta=2.044$, and $\tau=379$.

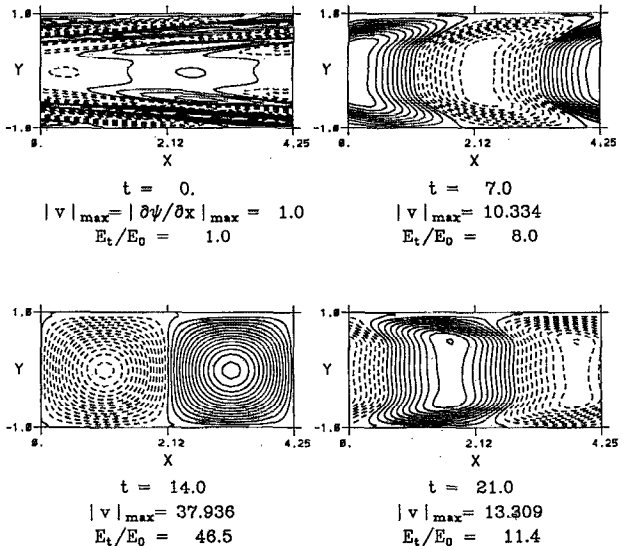

FIG. 15. Development of the perturbation streamfunction ψ for the best growing 2-D energy optimal in Poiseuille flow with $R=5000$, located at $\alpha=1.48$, $\tau=14.1$.

Fig. 11 along with the bound defined by Howard in Eq. (26). Note that the optimal excitation bound predicts absolute stability for $R<20.7$, in agreement with Joseph.

Using the optimal excitation technique, we can also sketch out curves in wave-number space that define regions of absolute stability, outside of which no perturbations can grow. Figure 12 shows these zero growth curves for Reynolds numbers of 21, 1000, and 4000. Also plotted are $100\times$ curves for $R=1000$ and 4000, within which perturbations capable of energy growth of two orders of magnitude or more are possible. The zero growth curve for $R=21$ encloses the spanwise disturbance with $\beta=1.56$ associated with Joseph's minimum critical Reynolds number.

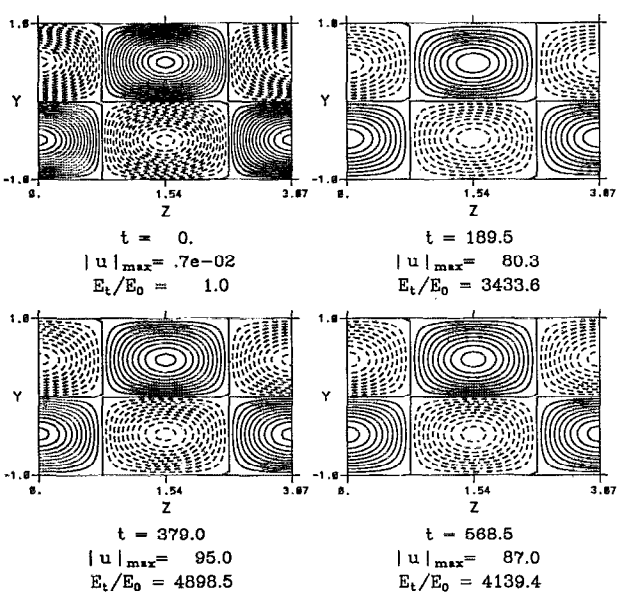

FIG. 14. Development of the perturbation streamwise velocity u for the global optimal in Poiseuille flow with $R=5000$, located at $\alpha=0$, $\beta=2.044$, and $\tau=379$. Values are normalized by the maximum value of v at time $t=0$.

It is clear on exploring wave-number space for growing perturbations that the optimal energy growth is a smooth function of time and wave number. This raises a question of the relative importance of locations in (α,β,R) space at which resonance between a single Orr–Sommerfeld mode and a single Squire mode generates an algebraic growth term. To see whether resonance is descriptive of the optimal perturbation at a resonance point, we consider the optimal at $R=125$, $\alpha=0.095\,64$, and $\beta=2.4982$ (equivalent to the $R=500$, $k=5$ resonance point in the geometry used by Gustavsson and Hultgren[15]). The eigenvalues for the first Orr–Sommerfeld and Squire modes are indeed equivalent for this problem, with $c_i=1.036$, and the optimal excitation does indeed select this resonance, assigning these two modes coefficients two orders of magnitude greater than any other mode. The maximum energy growth attained by this perturbation is 14 times its initial energy at $\tau=12$. When we move away from this point in wave-number space, however, the energy growth does not drop off, as would occur if resonance between two modes were the only mechanism for obtaining growth in the flow. Instead, similar or improved energy growth is obtained by shifting the weight of the coefficients to other modes. The best growth available for this Reynolds number is achieved by a perturbation with $\alpha=0.144$ and $\beta=1.63$, which grows by a factor of 18.6 in 16 advective time units.

IV. OPTIMAL PERTURBATIONS IN POISEUILLE FLOW

In Poiseuille flow, the global optimal perturbation is found to be a streamwise vortex, with $\alpha=0$. Maximum

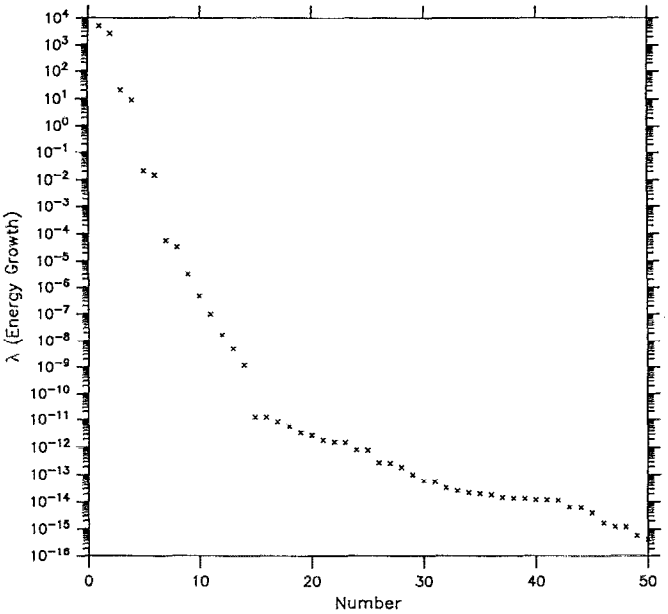

FIG. 16. Energy growth eigenvalues for the global optimal in Poiseuille flow with $R=5000$, showing that there are two strongly growing perturbation types.

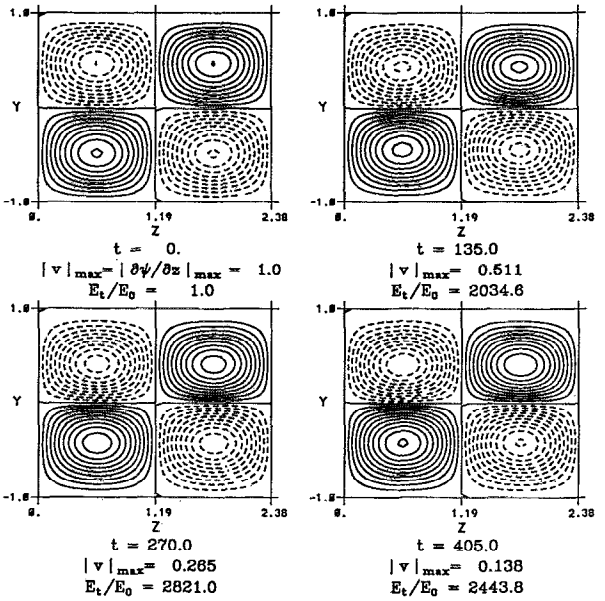

FIG. 17. Development of the perturbation streamfunction ψ for the best growing symmetric optimal in Poiseuille flow with $R=5000$, located at $\alpha=0$, $\beta=2.644$, and $\tau=270$.

energy growth for $R=5000$ is determined to be 4897 times the initial energy, reached in 379 advective time units for a spanwise-varying perturbation with $\beta=2.044$. The development of streamfunction and streamwise velocity for this perturbation are shown in Figs. 13 and 14; note that the parabolic shape of the mean flow leads to the growth of u in antisymmetric pairs of peaks about the $y=0$ axis. The best 2-D optimal for the same flow (Fig. 15) grows by only 46 times over 14 time units. As with Couette flow, the 3-D perturbations which gain the most energy over shorter time periods have shorter streamwise wavelengths to take advantage of the 2-D Reynolds stress growth mechanism.

Figure 16 shows the optimal growth eigenvalues, ordered in magnitude, for the Poiseuille flow global optimal at $R=5000$, $\alpha=0$, and $\beta=2.044$. Unlike Couette flow, Poiseuille flow supports a second set of strongly growing perturbations, whose energy growths are roughly half of those of the best energy optimals. This class of optimals, the strongest growing of which is shown in Figs. 17 and 18, fits two streamwise vortices into the channel width, resulting in symmetric peaks in u.

Table III shows the maximum energy growth for the global optimals, the strongest optimals over shorter time periods, and the best two-dimensional optimal. The peak energies for the antisymmetric and symmetric global optimals are compared in this table to those found analytically by Gustavsson[21] for perturbations with zero initial normal vorticity forced by the least-damped symmetric and antisymmetric Orr–Sommerfeld modes, respectively. This latter approach has apparently captured much of the energy growth capability of the best-growing perturbation. The modal spectral projection of the antisymmetric global optimal indicates that a contribution is also made by the second-least-damped Orr–Sommerfeld mode, with smaller contributions from the third- and fourth-least-damped modes.

The perturbations which will be observed in a laboratory flow depend on the initial conditions themselves as well as on their growth potential. The geometry or interior noise in an experiment may select perturbations that grow robustly but not necessarily optimally. For example, the

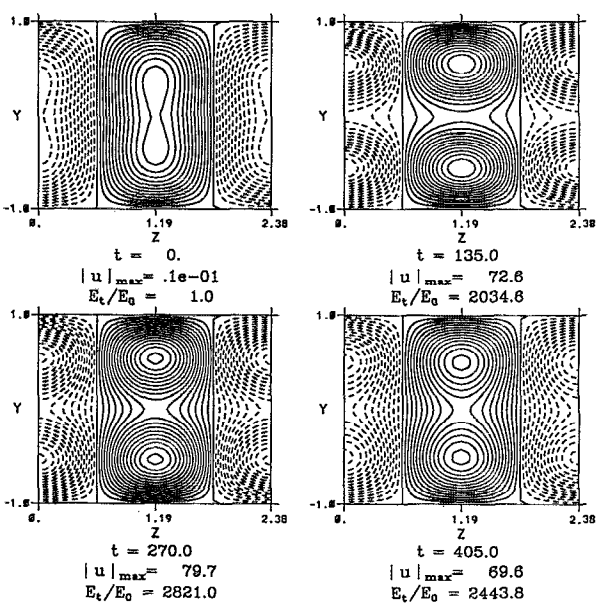

FIG. 18. Development of the perturbation streamwise velocity u for the best growing symmetric optimal in Poiseuille flow with $R=5000$, located at $\alpha=0$, $\beta=2.644$, and $\tau=270$. Values are normalized by the maximum value of v at time $t=0$.

TABLE III. Optimal perturbations in Poiseuille flow at $R=5000$.

	τ	α	β	E_τ/E_0
Antisymmetric global optimal	379	0	2.044	4897
Gustavsson—antisymmetric peak	420	0	1.98	4448
Symmetric global optimal	270	0	2.644	2819
Gustavsson—symmetric peak	286	0	2.60	2708
Best optimal at $\tau=20$	20	0.93	3.1	512
Best optimal at $\tau=5$	5	3.6	7.3	49.1
Best 2-D optimal	14.1	1.48	0	45.7

experimental spanwise variations whose effects were investigated by Asai and Nishioka[6] are symmetric in y, and are thus reminiscent of the second class of energy optimals for Poiseuille flow described here.

V. OPTIMAL PERTURBATIONS IN A BLASIUS BOUNDARY LAYER

Clearly the vortex-tilting and Reynolds stress mechanisms are capable of generating growth of perturbations in any sufficiently inviscid shear flow. A third shear flow profile of interest is the Blasius profile, which represents a boundary-layer flow.

For the semi-infinite domain of a boundary-layer flow, the number of discrete modes is finite, and a continuous spectrum is required to represent an arbitrary initial condition.[40] The normal velocity component of a disturbance which is independent of the streamwise coordinate x consists solely of the continuous spectrum.[17] Results for Couette and Poiseuille flow, however, lead us to anticipate that the optimal perturbations in this flow will be confined to the shear region near the wall. The Blasius boundary layer is therefore modeled as a channel flow with channel width sufficient to adequately represent the optimal perturbation. Increasing the channel width above some level for a given optimal perturbation, keeping discretization fixed, is indeed found to leave the energy growth eigenvalues unchanged. This level is selected as the proper channel width for this perturbation, and the continuous spectrum is represented as the discrete set of modes for that channel. The energy growth eigenvalues are also found to converge to the same values when the upper no-slip channel wall boundary is replaced with the traditional Blasius upper boundary condition of $v\sim\exp(-ky)$.

For simplicity, parallel flow is assumed. The Reynolds number, R_δ, is based on the free-stream velocity U_0 and the displacement thickness $\delta_1=1.7208(\nu x_0/U_0)^{1/2}$, where x_0 is the distance downstream from the leading edge of the plate. The Orr–Sommerfeld eigenproblem for Blasius flow was verified by comparison to Jordinson's results for temporal modes.[41]

The global optimals for this flow are streamwise vortices. For $R_\delta=1000$, the global optimal has spanwise wave number $\beta=0.65$ and growth time $\tau=778$, at which time its energy has increased by a factor of 1514. Streamfunction and streamwise velocity plots are shown in Figs. 19 and 20. The location of maximum streamwise velocity growth is closer to the wall than the location of maximum normal

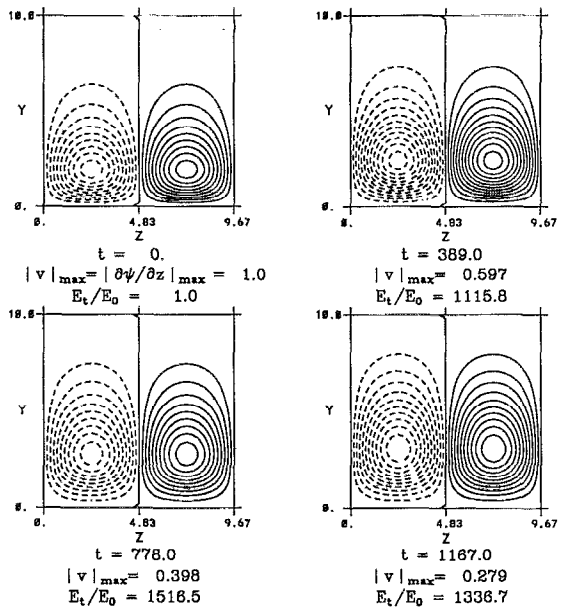

FIG. 19. Development of the perturbation streamfunction ψ for the global optimal in Blasius flow with $R_\delta=1000$, located at $\alpha=0$, $\beta=0.65$, and $\tau=778$.

velocity v. This concurs with the observation of Hultgren and Gustavsson[17] that such an effect is to be expected for elongated structures in boundary-layer flow, since, as demonstrated in (1), the rapid growth of u in time is due to the vU' term and U' is decreasing rapidly away from the wall.

Figure 21 presents a plot of the energy growth eigenvalues λ for the optimal perturbation in Blasius flow. A comparison of the energy growth of the strongest-growing

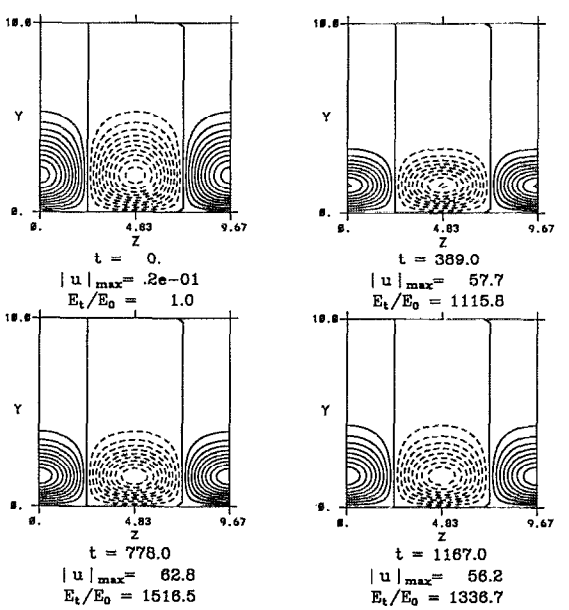

FIG. 20. Development of the perturbation streamwise velocity u for the global optimal in Blasius flow with $R_\delta=1000$, located at $\alpha=0$, $\beta=0.65$, and $\tau=778$. Values are normalized by the maximum value of v at time $t=0$.

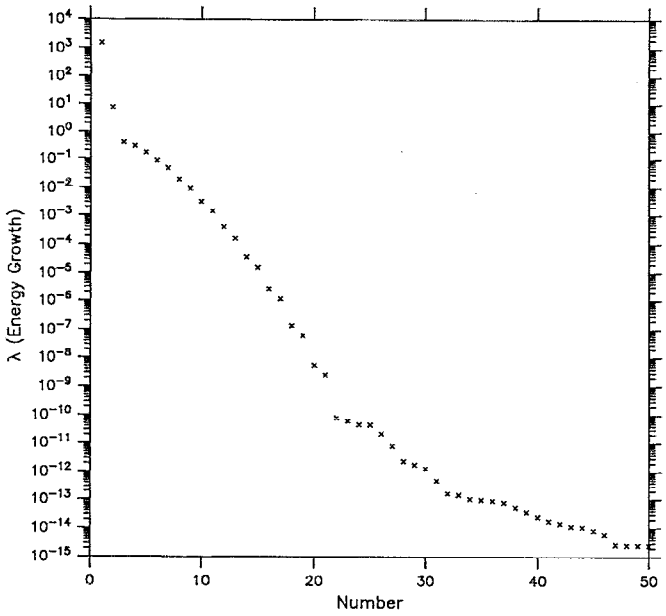

FIG. 21. Energy growth eigenvalues for the global optimal in Blasius flow with $R_\delta = 1000$, showing that the energy growth of the next most potent perturbation is two orders of magnitude smaller.

disturbance to the energy growth of the other disturbances suggests that other types of perturbations are much less likely to appear in a boundary-layer flow.

The optimal perturbations for Blasius flow are found to share many characteristics with optimals from Couette and Poiseuille flows. For global optimals, the spanwise wave number is independent of R_δ at $\beta = 0.65$, the time period τ for maximum energy growth scales with R_δ, and the maximum energy growth, E_τ/E_0, scales with R_δ^2. Table IV compares the statistics of the global optimal with those of optimals with shorter growth periods and the best 2-D optimal, which is again found to produce much less growth than the 3-D elongated optimal disturbances with variations in the cross-stream direction.

VI. DISCUSSION

The streamwise vortex, which emerges from the three-dimensional optimal perturbation problem as the disturbance capable of the greatest energy growth, has interesting properties. The streamwise vorticity components are decoupled from the large increases in streamwise velocity u, and are capable only of decay. By itself, the streamwise vortex is passive to nonlinear development, as pointed out by Gustavsson.[21] However, the ubiquity of streaks in experiments, manifested as spanwise variations in streamwise velocity, indicates that perturbations elongated in the streamwise direction are generally present in the background noise. Once generated, perturbations with streamwise vorticity have a profound effect on the flow through the development of powerful streaks. These streaks may themselves be unstable to secondary instabilities, or they may provide a base for strong transient growth of other types of perturbations.

TABLE IV. Optimal perturbations in Blasius flow at $R_\delta = 1000$.

	τ	α	β	E_τ/E_0
Global optimal	778	0	0.65	1514
Best optimal at $\tau = 100$	100	0.15	0.96	652
Best optimal at $\tau = 20$	20	0.87	1.7	78
Best 2-D optimal	45	0.42	0	28

Since there is a limited subset of perturbation types that grow robustly in a shear flow, we expect to see streaks generated by the streamwise vortex recur frequently and persistently. It is not surprising that experimentalists encounter difficulties in eliminating these streaks from their experiments.

Traditional instability theory assumes the perturbation of importance in a flow is the mode of the associated linearized dynamic system with largest exponential growth rate. The problem with this approach is that it fails to take account of the fact that the equations that describe the development of a small disturbance are not self-adjoint. From a modal perspective, growth results when initially the nonorthogonal modes destructively interfere, then separate as they evolve to constructively interfere, potentially revealing large growth. The very slow growth of the exponentially growing mode for Poiseuille flow at high Reynolds numbers (maximum energy growth rate of $2\sigma \sim 0.015$), and the decay of all modes for Poiseuille flow below $R_c \simeq 5772$ and for Couette flow at all R make no practical difference in the types of perturbations which grow the most in these flows. It is perhaps more instructive in these types of problems to talk about physical mechanisms of growth, such as vortex tilting and down-gradient momentum flux due to Reynolds stress, than to consider the problem in terms of modal structure.

The failure to take the nonorthogonality of the modes of the linearized dynamical system into account can lead to some misleading conclusions about the behavior of small disturbances in a parallel shear flow. Squire's theorem, which requires the growth of a three-dimensional modal perturbation to be less than that of an associated two-dimensional modal perturbation at a smaller Reynolds number,[4] appears to justify concentrating on 2-D disturbances while ignoring 3-D disturbances in the linear analysis. The problem with this interpretation arises from the implicit limitation of Squire's theorem to consideration of a single mode. An arbitrary initial condition is actually made up of many nonorthogonal modes, the combination of which can result in far more dramatic growth for 3-D linear disturbances than for 2-D disturbances, as this work demonstrates.

The growth of three-dimensional secondary instabilities on a two-dimensional basic flow has been widely studied as a possible path to turbulence.[42] This theory relies on the existence of a steady or quasisteady finite-amplitude 2-D structure in the flow, whose origin for subcritical Reynolds numbers must involve a finite initial disturbance. The potential for 2-D optimal perturbations to provide the required 2-D basic flow on a rapid (advective) time scale was suggested by Farrell's[14] linear study and verified nonlin-

early by Butler.[22,43] However, comparison of the energy growth of the best 2-D optimal perturbations to that of the best 3-D optimals (see Fig. 8 and Tables I, III, and IV) strongly favors the 3-D structure. It would be interesting to explore the nature of secondary instability growth on basic flows suggested by the types of disturbances shown to result from optimal perturbation theory.

In order to discuss the potential contribution of the initial-value problem to transition to turbulence in viscous shear flows, we must consider finite-amplitude disturbances. Because of this limitation, the importance of transient behavior has often been overlooked. This same limitation applies, however, when we use classical instability theory to try to explain the behavior of real fluids. We are not as interested in infinitesimal disturbances as we are in the nonlinear turbulent or equilibrated flow that emerges in a finite time. In problems for which the fastest growing instability has a large growth rate (i.e., comparable to the inverse of the advective time scale), the behavior during early stages of transition to turbulence is often well described by instability theory. Channel flows, with primary exponential modes corresponding to instabilities that grow on viscous scales or are in fact least-damped decaying disturbances, are not such problems. Experiments demonstrate the sensitivity of these flows to the level of noise in the apparatus. Understanding of these flows may be best approached by considering the types of perturbations that grow the most robustly.

The optimal perturbation technique has provided us with examples of small disturbances that grow rapidly and robustly in a specified mean shear flow. Even if the exact optimal initial conditions are not reproduced in a real flow, we have found the characteristics of disturbances that can be expected to grow well; namely, these disturbances are elongated in the streamwise direction with spanwise widths comparable with the width of the shear layer, they have streamwise vorticity, and they may have phase orientation opposite that of the mean shear. The slow variation of optimal energy growth with wave number suggests that biases in the spectrum of the imposed perturbation field in a given experimental apparatus can play a significant role in selecting wave numbers of perturbations active in the early stages of transition, as the wave numbers defining the global optimal for a flow are not strongly preferred. The distribution and amplitude of such initial conditions in a flow due to interior stochastic driving or to boundary forcing is an interesting topic for future research, as is the susceptibility of these disturbances to secondary growth of other perturbations.

ACKNOWLEDGMENTS

We would like to thank Professor Dan Henningson, Professor L. Håkan Gustavsson, Dr. Satish C. Reddy, and Dr. Petros Ioannou for helpful discussions.

This work was supported by National Science Foundation Grant No. ATM-8912432, with computer time provided by NCSA Grant No. ATM-900015N and NCAR Grant No. 35121031. The National Center for Atmospheric Research is supported by the National Science Foundation. Support from the Zonta International Amelia Earhart Fellowship and the Robert L. Wallace Prize Fellowship is also gratefully acknowledged.

[1] S. J. Davies and C. M. White, "An experimental study of the flow of water in pipes of rectangular section," Proc. R. Soc. London Ser. A **119**, 92 (1928).

[2] M. Nishioka, S. Iida, and Y. Ichikawa, "An experimental investigation of the stability of plane Poiseuille flow," J. Fluid Mech. **72**, 731 (1975).

[3] N. Tillmark and P. H. Alfredsson, "Experiments on transition in plane Couette flow,"J. Fluid Mech. **235**, 89 (1992).

[4] H. B. Squire, "On the stability for three-dimensional disturbances of viscous fluid flow between parallel walls," Proc. R. Soc. London Ser. A **142**, 621 (1933).

[5] P. S. Klebanoff, K. D. Tidstrom, and L. M. Sargent, "The three-dimensional nature of boundary-layer instability," J. Fluid Mech. **12**, 1 (1962).

[6] M. Asai and M. Nishioka, "Origin of the peak–valley wave structure leading to wall turbulence," J. Fluid Mech. **208**, 1 (1989).

[7] W. Thomson, "Stability of fluid motion—Rectilineal motion of viscous fluid between two parallel planes," Philos. Mag. **24**, 188 (1887).

[8] T. Ellingsen and E. Palm, "Stability of linear flow," Phys. Fluids **18**, 487 (1975).

[9] M. T. Landahl, "Wave breakdown and turbulence," SIAM J. Appl. Math. **28**, 735 (1975).

[10] M. T. Landahl, "A note on an algebraic instability of inviscid parallel shear flows," J. Fluid Mech. **98**, 243 (1980).

[11] D. S. Henningson, "The inviscid initial value problem for a piecewise linear mean flow," Stud. Appl. Math. **78**, 31 (1988).

[12] K. S. Breuer and J. H. Haritonidis, "The evolution of a localized disturbance in a laminar boundary layer. Part 1. Weak disturbances," J. Fluid Mech. **220**, 569 (1990).

[13] J. Pedlosky, *Geophysical Fluid Dynamics*, 2nd ed. (Springer-Verlag, New York, 1987), Sec. 7.3.

[14] B. F. Farrell, "Optimal excitation of perturbations in viscous shear flow," Phys. Fluids **31**, 2093 (1988).

[15] L. H. Gustavsson and L. S. Hultgren, "A resonance mechanism in plane Couette flow," J. Fluid Mech. **98**, 149 (1980).

[16] L. H. Gustavsson, "Resonant growth of three-dimensional disturbances in plane Poiseuille flow," J. Fluid Mech. **112**, 253 (1981).

[17] L. S. Hultgren and L. H. Gustavsson, "Algebraic growth of disturbances in a laminar boundary layer," Phys. Fluids **24**, 1000 (1981).

[18] D. J. Benney and L. H. Gustavsson, "A new mechanism for linear and nonlinear hydrodynamic instability," Stud. Appl. Math. **64**, 185 (1981).

[19] P. S. Jang, D. J. Benney, and R. L. Gran, "On the origin of streamwise vortices in a turbulent boundary layer," J. Fluid Mech. **169**, 109 (1986).

[20] L. H. Gustavsson, "Excitation of direct resonances in plane Poiseuille flow," Stud. Appl. Math. **75**, 227 (1986).

[21] L. H. Gustavsson, "Energy growth of three-dimensional disturbances in plane Poiseuille flow," J. Fluid Mech. **224**, 241 (1991).

[22] K. M. Butler, "Equilibration and optimal excitation in viscous shear flow," Ph.D. thesis, Harvard University, 1991.

[23] C. C. Lin, "Some mathematical problems in the theory of the stability of parallel flows," J. Fluid Mech. **10**, 430 (1961).

[24] I. V. Schensted, "Contributions to the theory of hydrodynamic stability," Ph.D. thesis, University of Michigan, 1960.

[25] R. C. DiPrima and G. J. Habetler, "A completeness theorem for non-self-adjoint eigenvalue problems in hydrodynamic stability," Arch. Rat. Mech. Anal. **34**, 218 (1969).

[26] S. C. Reddy, P. J. Schmid, and D. S. Henningson, "Pseudospectra of the Orr–Sommerfeld operator," SIAM J. Appl. Math. (in press).

[27] I. Percival and D. Richards, *Introduction to Dynamics* (Cambridge U.P., New York, 1982).

[28] B. F. Farrell and A. M. Moore, "An adjoint method for obtaining the most rapidly growing perturbation to oceanic flows," J. Phys. Ocean. **22**, 338 (1992).

[29] S. A. Orszag, "Accurate solution of the Orr–Sommerfeld stability equation," J. Fluid Mech. **50**, 689 (1971).

[30] A. Davey and W. H. Reid, "On the stability of stratified viscous plane Couette flow. Part 1. Constant buoyancy frequency," J. Fluid Mech. **80**, 509 (1977).

[31] D. Henningson (private communication, 1991).

[32]W. H. Press, B. P. Flannery, S. A. Teukolsky, and W. T. Vetterling, *Numerical Recipes: The Art of Scientific Computing* (Cambridge U.P., New York, 1986).
[33]J. Kim and R. D. Moser, "On the secondary instability in plane Poiseuille flow," Phys. Fluids A **1**, 775 (1989).
[34]Z. Yang, "A single streamwise vortical structure and its instability in shear flows," Ph.D. thesis, Harvard University, 1988.
[35]J. Hamilton, "Streamwise vortices and transition to turbulence," Ph.D. thesis, Harvard University, 1991.
[36]O. Reynolds, "On the dynamical theory of incompressible viscous fluids and the determination of the criterion," Philos. Trans. R. Soc. London Ser. A **186**, 123 (1895).
[37]J. Serrin, "On the stability of viscous fluid motions," Arch. Rat. Mech. Anal. **3**, 1 (1959).
[38]L. N. Howard, "Bounds on flow quantities," Annu. Rev. Fluid Mech. **4**, 473 (1972).
[39]D. D. Joseph, "Nonlinear stability of the Boussinesq equations by the method of energy," Arch. Rat. Mech. Anal. **22**, 163 (1966).
[40]L. M. Mack, "A numerical study of the temporal eigenvalue spectrum of the Blasius boundary layer," J. Fluid Mech. **73**, 497 (1976).
[41]R. Jordinson, "Spectrum of eigenvalues of the Orr–Sommerfeld equation for Blasius flow," Phys. Fluids **14**, 2535 (1971).
[42]B. J. Bayly, S. A. Orszag, and T. Herbert, "Instability mechanisms in shear-flow transition," Annu. Rev. Fluid Mech. **20**, 359 (1988).
[43]K. M. Butler and B. F. Farrell, "Efficient excitation of elliptical vortices in plane channel flow," American Physical Society, Division of Fluid Mechanics 43rd Annual Meeting, 18–20 November 1990.